ORIGINAL ARTICLE

Torrefaction of agro-wastes (palmyra palm shell and redgram stalk): characterization of the physicochemical properties and mechanical strength of binderless pellets

Vallu Ramakrishna[1] · Ashok K. Singh[1] · G. K. Bayen[1] · R. E. Masto[1] · R. K. Meena[1] · Pradeep K. Singh[1] · M. Arya[1] · S. Jyoti[1] · Arnold L Usham[1]

Abstract

To increase the utilization of agro-waste as solid fuel, torrefaction is an important process to improve the fuel properties. In the present investigation, palmyra palm shell (PPS) and redgram stalk (RS) were torrefied in a specially designed stainless-steel tubular reactor with varying temperatures (230 °C, 260 °C, and 300 °C) under a nitrogen atmosphere at two residence times of 30 and 60 min. The influence of torrefaction temperature and residence time on mechanical properties and moisture reabsorption tendency of the binderless pellets were investigated. With increasing the torrefaction temperature up to 300 °C (60-min residence), the mass and energy yield decreased, and the fixed carbon, high heating value, and energy density increased. The fuel ratio (FR) increased from 0.25 or 0.23 to 1.35 and 0.52 for PPS and RS, respectively. The combustibility index increased up to a certain temperature (260 °C); however, at 300 °C, it decreased. Grindability of the torrefied biomass increased; about 99.89% and 95.28% of the smallest particles' fraction pass through a < 75-µm sieve for PPS and RS, respectively, at 300 °C and 60 min as compared to the raw agro-wastes. The moisture reabsorption tendency of untorrefied and torrefied PPS and RS pellets was measured under the controlled environment of 60% RH at 40 °C. FTIR study supported the hydrophobicity of the torrefied material than the raw biomass. This study demonstrated that the torrefied PPS and RS have fuel properties comparable with India lignite, and this renewable fuel could be sustainably used for power generation and domestic applications.

Keywords Agro-waste–torrefaction · Energy density · Combustion indices · Higher heating value · Grindability · Mechanical properties

1 Introduction

According to the Indian Ministry of New and Renewable Energy (MNRE), around 350 million tonnes of agro-wastes are generated annually [1]. About 92 million tonnes of agro-wastes are being burned incompletely, and the remaining waste is surplus. Agro-waste is associated with several disadvantages such as high moisture content, high volatile matter, low carbon content, low energy density, high fibrous nature, and poor grindability [2–4]. However, agro-waste

has the potentiality to generate electricity [5] and for use in steel-making [6] and building materials [7]. The use of biomass for pyrolysis [8, 9], gasification [10, 11], and combustion [12, 13] is affected by some unfavorable physical and chemical properties. Therefore, it is required to improve the fuel quality of agro-waste by pre-treatment. Torrefaction is a well-known pre-treatment technique for improving the quality of biomass. It involves heating the biomass at 200–300 °C in an inert atmosphere [14]. At this temperature, biomass undergoes partial decomposition. The torrefaction is also called as mild pyrolysis [15] process. Torrefied biomass has improved its quality in terms of higher energy density or heating value [16, 17], fixed carbon content, fuel ratio [18], hydrophobicity[19, 20], lower atomic O/C, and H/C ratios [21, 22]. The fibrous nature of biomass consumes more energy during the grinding process. However, torrefaction improves grindability [23, 24] and decreases the energy

✉ Vallu Ramakrishna
vcramakrishna06@gmail.com

1 CCS RQA Research Group, CSIR-Central Institute of Mining and Fuel Research, Digwadih Campus, Dhanbad, Jharkhand 828108, India

consumption by 40–88% as compared to the raw biomass [25], which is essential for co-firing with coal power generation. Bridgeman et al. [26] investigated that the Hardgrove grindability index of pulverizing behavior of some of the torrefied biomass samples was not reliable as coal sample grinding behavior. Particle size distribution provides more accurate information about the grinding behavior [27]. The torrefaction temperature influence on the physicochemical properties of pigeon pea (redgram) stalk has been studied by Singh et al. [28] and found that the char yield for TPS-275–45 was 40.4%. However, the energy yield is very low (0.50), and such high-temperature torrefaction is non-beneficial for pigeon pea stalk. Chen et al. [14] reported that the higher heating value (HHV) of torrefied rice husk increased from 16.79 MJ/kg for rice husk (RH) to 18.9 MJ/kg for RH-300 and a lower HHV was obtained in oxidative torrefaction than non-oxidative torrefaction due to the loss of some carbon and hydrogen during oxidative torrefaction. However, at a fixed torrefaction temperature, there is no impact of O_2 concentration on the HHV of torrefied rice husk. Therefore fuel properties of rice husk are more sensitive to temperature than O_2 concentration. Torrefaction processes have been proven to improve the physicochemical properties of biomass for further utilization in several applications.

However, loosen torrefied biomass has some issues related to the dust explosion and self-ignition during transportation and storage as compared to torrefied biomass pellets. Torrefied pellets have been widely used in various fields of boiler combustion, heating, and power generation [29, 30]. However, the bulk density of torrefied biomass is often poor and lower than biomass; as a result, it poses challenges for storage, transportation, and economic feasibility [31–33]. In order to use the torrefied biomass effectively as a universally traded bioenergy commodity, the torrefied biomass should be densified. The currently available densified technique is known as pelletization [34]. Universal demand for torrefied pellets increases day by day. It is expected to increase twofold by 2024 from 24.5 to 50 million metric tons [35]. Pelleting enhances production efficiency and transportation and reduces operational costs, thus increasing economic and energetic feasibility [36]. Ghiasi et al. [37] prepared torrefied pellets by two different process routes, i.e., first pellets were prepared followed by torrefaction (scheme-I) or torrefaction followed by pelletization (scheme-II) to convert Douglas-fir wood chips to torrefied wood pellets. For scheme-II, the pellets were more hydrophobic, with higher density, heating value, and carbon content. Yang et al. [38] developed a technology for synchronized torrefaction and pelleting (STP) with ultrasonic vibration. Two fuel upgrading processes (torrefaction and pelletization) have happened simultaneously with the assistance of ultrasonic vibration. STP was effective for enhancing the density and durability

of torrefied biomass pellets. Liu et al. [39] prepared two types of pellets from biomass and corresponding hydro char. The fuel quality of hydro char pellets has high mechanical strength, low moisture uptake, and improved combustion property, which indicated that hydro char pellets were more suitable than raw biomass pellets as solid biofuel. Chen et al. [40] reported that the up-gradation of biomass pellets by torrefaction and observed that higher temperature torrefaction affects the pellet's strength. It was suggested that the torrefaction temperature between 250 and 300 °C is suitable for pellets.

So far, great works have been done on the physicochemical properties of torrefied biomass. However, the influence of torrefaction temperature on the mechanical properties and moisture reabsorption tendency of torrefied binderless pellets are limited [37, 40]. Further, the palmyra and redgram residues are not studied in detail. Currently, palmyra palm shells and redgram stalks are being used as solid biofuels. India has the highest palmyra palm (102 million) production. Redgram is cultivated in 3.9 million hectares in India and 5.4 million hectares in the world.

The objective of this study was to produce fuel pellets from the biomass wastes of palmyra palm and redgram by integrating torrefaction and pelletization processes. The impact of torrefaction temperature and residence time on the mass and energy yields, mechanical properties, and moisture reabsorption tendency of the fuel was studied in detail to supply some fundamental data for the application of palmyra and redgram residue pellets. The palmyra palm shell (PPS) and redgram stalk (RS) pellets were prepared by torrefaction followed by pelletization without any binder use as shown in Fig. 1.

2 Materials and methods

2.1 Materials

Redgram stalks (RSs) were collected from Nandarada village (Near Rajahmundry, AP), and palmyra palm shells (PPSs) were collected from CSIR-Central Institute of Mining and Fuel Research colony, Digwadih, Jharkhand. About 5 kg of PPS and RS were cut into 1 cm pieces and stored in a polythene bag for further torrefaction studies. Before torrefaction, the small pieces of PPS and RS were dried at 105 °C for 24 h.

2.1.1 Identification of agro-wastes (materials)

In the present study, the untorrefied palmyra palm shell and redgram stalks have been designated as PPS and RS. Torrefied PPS and RS samples were labeled as PPS-K-L and RS-K-L [28, 40]. The parameter K specifies the torrefaction

Fig. 1 Schematic route for the preparation of pellets from PPS and RS

temperature, and L indicates residence time. For instance, PPS-230–30 is designated as the PPS torrefied at 230 °C with 30-min residence time. Other fractions of torrefied agro-wastes were also mentioned in a similar way, i.e., PPS-230–30, PPS-230–60, PPS-260–30, PPS-260–60, PPS-300–30, and PPS-300–60. RS-230–30, RS-230–60, RS-260–30, RS-260–30, RS-300–30, RS-300–60, and RS-230–30 mean 230 °C with 30 min of the residence time, and other fractions of temperature and time also mentioned similarly, i.e., 230–60, 260–30, 260–60, 300–30, and 300–60; UT referred to as untorrefied. PPS and RS is referred to as agro-wastes.

2.2 Torrefaction reactor

Torrefaction experiment was carried out in a stainless steel tubular reactor of 400-mm length and 100-mm diameter. The reactor with a measured quantity of agro-waste was placed into an electrical muffle furnace through the front door. Nitrogen gas flow was arranged into the reactor to create an inert atmosphere before heating the PPS and RS. Two thermocouples were placed inside the stainless steel reactor for monitoring the sample temperature. The temperature of the furnace was controlled by the temperature control unit of the furnace. A digital pyrometer (source: iron constant) has been used to crosscheck the sample's temperature.

2.2.1 Torrefaction experiment

About 300 g of 1-cm size PPS and RS were torrefied at different temperatures (230 °C, 260 °C, and 300 °C) and residence time (30 and 60 min) in a sealed tubular reactor. Nitrogen gas was purged at the rate of 1 L/min into the reactor before heating and during the torrefaction process. The temperature of the reactor was increased at the rate of 5 °C/min. After reaching the required temperature, heating

was continued for 30 and 60 min and then cooled down to room temperature by keeping the nitrogen gas flowing into the reactor at the same rate. Subsequently, PPS and RS yield was determined. The torrefied PPS and RS were stored in sealed polythene bags and kept in a desiccator for further experiments.

2.3 Characterization of PPS and RS

PPS and RS were characterized as per the procedure described in the ASTM standards; ASTM-E871, ASTM-E1755, and ASTM-E872 were followed for the analysis of moisture (%), ash (%), and the volatile matter (%), respectively. The gross calorific value of PPS and RS were determined with the aid of a bomb calorimeter, model PARR 6400, as per the ASTM D5865.

2.3.1 Combustion indices

In order to examine the effect of the torrefaction on the combustion indices, parameters such as fuel ratio (FR), combustion index (CI), and volatile ignitability (VI) were calculated using heating value, ash content, volatile matter, and fixed carbon of untorrefied and torrefied PPS and RS. Combustion indices parameters were calculated using Eqs, 1–3:

Fuel ratio (FR) : $FR \dfrac{FC_{db}}{VM_{db}}$ (1)

where FC_{db} is fixed carbon (dry basis) and VM_{db} volatile matter (dry basis).

Combustion index (CI) : $CI = HHV_{db} \times \left(115 - Ash_{db}\right) \times \dfrac{1}{105 \times FR}$ (2)

where CI is in MJ/kg and Ash db content in biomass on a dry basis.

Volatile ignitability (VI)：$VI = \frac{HHV_{db} - 0.338FC_{db}}{VM_{db} - M_{db}} \times 100$ (3)

where VI is in MJ/kg, VM_{db} is volatile matter (%) in biomass on dry basis, FC_{db} is fixed carbon (%) on dry basis, and M_{db} is moisture (%) contenton dry basis.

The energy density ratio (MJ/kg) is calculated by using

$$\text{Energy density ratio} = \frac{HHV_T}{HHV_R} \qquad (4)$$

Higher heating value on dry basis (HHV_{db}) is calculated using

$$HHV_{db} = \frac{HHV_m \times 100}{100 - M} \qquad (5)$$

where M is moisture content in biomass.

Energy yield is calculated using Eq. 6:

$$Y_E = Y_M \times \frac{HHV_T}{HHV_R} \qquad (6)$$

where Y_M is mass yield, HHV_T is the higher heating value of torrefied PPS and RS, and HHV_R is the heating value of untorrefied PPS and RS.

2.3.2 FTIR analysis

IR Affinity-1S, SHIMADZU instrument, was used for the identification of functional groups of PPS and RS. Before analysis, the sample was prepared in tablet form by compressing 1–2 mg of a dried sample with *KBr*(200 mg). The frequency range was kept from 4000 to 400 cm^{-1}.

2.3.3 Grindability experiment

The grindability behavior of untorrefied and torrefied PPS and RS was established by the particle size distribution of the ground samples. The untorrefied and torrefied PPS and RS agro-wastes were ground with a mortar grinder, RETSCH, RM 200. The grinding of the PPS and RS was carried out in two stages. The first stage was the pre-grinding stage, and the second stage was the fine grinding stage. In the pre-grinding stage, particle sizes were reduced to 0.2–1.18 mm from 1 cm. In the second stage, 50 g of PPS and RS were ground for 15 min (100 rpm, 60 Hz) [27, 41]. The ground samples were sieved with five different-sized fractions, viz., < 75, 75–177, 177–425, 425–710, and 710–1000 μm, with the help of a sieve shaker for 30 min. Particle size distribution was carried out in the following

procedure for screen analysis and recorded as a cumulative mass percentage.

2.4 Preparation of pellets from torrefied PPS and RS agro-wastes

A single pellet press unit, hydraulic (KBr) bench Press (MODEL M-15) Techno Search Instruments, has been used to prepare the torrefied PPS and RS pellets. The pellet press contained a cylinder with 19.00-mm inside diameter and 66.00-mm height and a piston suitable to move into the cylinder. The end of the cylinder is closed with a removable backstop. About 2.0 g of each torrefied ground (< 36 mesh) PPS and RS was packed inside the cylinder without adding binder [35] and then manually compressed using about 5.50 and 10.30 tonnage of pressure upon the piston. A dwell time (i.e., the particles remain under the maximum compacting pressure during pelletization) of 20 s was chosen for all the experiments to minimize the pellet relaxation [42]. The pellets were removed from the cylinder by removing the backstop and pushing out by applying pressure on the pellet [39] and stored for 15 days in an airtight container at room temperature (approximately 30 °C) before characterization[43].

The mechanical properties of the untorrefied and torrefied PPS and RS pellets were analyzed by evaluating in terms of crushing strength and durability.

2.4.1 Crushing strength

The impact torrefaction on the crushing strength of biomass pellets was determined by gradually increasing the weight (0.5 kg in every increment) on the pellets until their breakage/fracture occurred. Average data of five pellets was used for crushing strength.

2.4.2 Durability (DUR)

To assess the PPS and RS pellets' durability, experiments were carried out by the following prescribed procedure of the "Roga Index test" for coal. About 2.0 g of the untorrefied and torrefied PPS and RS pellet(s) were introduced into a rotating Roga drum with a cover driving shaft transmission gear electric motor for carrying out the abrasion test. The drum has dimensions of 200-mm internal diameter, 70-mm depth, and a 2-mm-thick mild steel sheet. The drum is closed with a cover seated on a felt or rubber gasket and secured by four wing nuts. Two Roga drums are symmetrically mounted on a rotating driving shaft. Testing of two different pellets of the same sample with a duplicate was carried out in the machine. The drum was rotated with the stub axle horizontal at 50 ± 2 rev/min

with 1000 revolutions. After each stage of rotation, the sample was screened using a 3.15-mm sieve, and the particles smaller than 3.15 mm were weighed. The abrasion index, AI, was calculated from the mean value of duplication of the mass percentage of pellet below 3.15 mm relative to the total initial mass of PPS and RS pellets after 1000 revolutions in the rotary drum.

$$AI = (weight \ of \ the \ sample < 3.15 \ mm/initial \ weight \ of \ the \ sample) \times 100 \tag{7}$$

DUR $= 100 - AI$, where AI is the abrasiveness; < 3.15 mm is the mass of the particles smaller than 3.15 mm. Thus, the higher the AI values are, the lower the pellet's mechanical resistance. The higher the DUR means the quality of the pellets is better.

2.4.3 Effect of torrefaction on moisture reabsorption tendency of PPS and RS

About 2.0 g of torrefied and untorrefied PPS and RS pellets were placed in a 15-mL pre-dried moisture dish and kept in a hot air oven at 105 °C for 6 h to remove the inherent moisture. The dried pellets were then weighed and considered as the initial weight of the dry pellet. The moisture dishes containing the dry pellets were exposed to the controlled environment of 60% relative humidity (RH) at 40 °C using one volume sulfuric acid and 2.9 volume distilled water mixture into a desiccator. The desiccator and the contents were kept in a humidity chamber and maintained at 40 °C temperature for 120 h and weighed. The PPS and RS pellets were monitored at predetermined time intervals once every 24 h for 5 days. A hygrometer was used for monitoring the humidity of the mixture of the solution when the pellets were weighed in a predetermined time interval. The increase in weight of the PPS and RS was then taken as the moisture reabsorbed by the pellets.

3 Results and discussion

The work process flow chart of PPS and RS (Supplementary information S1) and various untorrefied and torrefied PPS and RS agro-wastes are shown in Fig. 2.

The PPS color appeared as brown to black, whereas RS changed its color from yellow to brown as the torrefaction temperature increased from 230 to 300 °C with 30 and 60 min of residence time. The change of color is related to the slow evaporation of inherent moisture and volatile matter. As increasing the severity of torrefaction, energy yield decreased significantly for PPS and RS as energy yield strongly depends on the mass yield. It may be due to the decomposition of the biomass's chemical structure by the loss of volatile compounds into H_2O, CO, and CO_2 [39, 42, 43]. The relative differences in mass yield were presumably due to loss of moisture, volatile matter, and substantial degradation of hemicellulose and cellulose. Other researchers observed similar results where mass and energy yields were decreased with the severity of torrefied temperature [14]. The faster devolatilization rate of volatile compounds increases the torgas yield with increased temperature and time [44]. The mass yields of the untorrefied and torrefied PPS and RS are shown in Table 2.

Fig. 2 Physical appearance of untorrefied and torrefied agro-wastes of palmyra palm shell (PPS) and redgram stalk (RS)

Table 1 Proximate analysis of untorrefied and torrefied PPS and RS on dry basis (db)

Untorrefied/torrefied agro-waste	Moisture (%)	Ash (%)	Volatile matter (%)	Fixed carbon (%)
PPS	7.43 (7.46)	0.71 (0.72)	79.50 (79.01)	19.79 (20.26)
PPS-230–30	6.75 (6.72)	1.03 (1.04)	76.36 (76.33)	22.61 (22.63)
PPS-230–60	6.50 (6.49)	1.05 (1.05)	74.04 (73.80)	24.91(25.15)
PPS-260–30	5.61(5.59)	1.33 (1.33)	65.67 (64.71)	33.1 (33.95)
PPS-260–60	5.39 (5.40)	1.40 (1.43)	62.98 (62.74)	35.68 (35.83)
PPS-300–30	4.91(4.93)	1.82 (1.83)	55.90 (55.75)	42.31 (42.42)
PPS-300–60	4.80 (4.78)	1.91 (1.93)	41.78 (40.96)	56.30 (57.13)
RS	7.54 (7.51)	1.08 (1.19)	80.28 (80.11)	18.64 (18.69)
RS-230–30	7.19 (7.17)	1.28 (1.29)	79.94 (79.87)	18.78 (18.83)
RS-230–60	6.60 (6.58)	1.35 (1.39)	76.10 (76.00)	22.55 (22.61)
RS-260–30	5.87 (5.85)	1.48 (1.58)	75.23 (73.91)	23.21 (24.50)
RS-260–60	5.57 (5.54)	1.69 (1.79)	74.72 (73.17)	23.54 (25.03)
RS-300–30	4.99 (4.96)	2.36 (2.39)	65.31(65.19)	32.31 (32.40)
RS-300–60	4.90 (4.88)	2.61 (2.63)	64.19 (63.63)	33.21 (33.73)

Table 2 Combustion indices parameters, mass yield, energy density ratio, and higher heating value(s) of PPS and RS on dry basis (db)

Agro-waste	Mass yield (%)	Energy yield (%)	HHV_{db} (MJ/kg)	Energy density ratio (MJ/kg)	Fuel ratio (FR)	Combustibility index (CI) (MJ/kg)	Volatile ignitability (VI) (MJ/kg)
PPS	—–	—–	19.50	—	0.25	85.27	17.93
PPS-230–30	77.00	78.49	19.88	1.02	0.30	72.90	17.71
PPS-230–60	75.00	76.66	19.94	1.02	0.34	64.31	17.17
PPS-260–30	65.00	74.17	22.25	1.14	0.50	47.83	18.54
PPS-260–60	60.00	71.41	23.21	1.19	0.57	44.32	19.50
PPS-300–30	55.00	66.88	23.72	1.22	0.76	33.77	18.60
PPS-300–60	45.00	58.35	25.29	1.30	1.35	20.21	17.03
RS	—	—	19.07	—	0.23	89.13	17.71
RS-230–30	87.42	89.18	19.45	1.02	0.23	89.67	18.15
RS-230–60	81.00	86.30	20.31	1.06	0.30	74.22	18.39
RS-260–30	79.00	84.25	20.33	1.06	0.31	71.26	17.94
RS-260–60	77.00	82.17	20.35	1.07	0.32	69.71	18.00
RS-300–30	67.00	80.00	22.71	1.19	0.49	49.24	19.62
RS-300–60	60.00	71.61	22.76	1.19	0.52	47.09	19.54

3.1 Effect of torrefaction on proximate analysis of PPS and RS agro-waste

Proximate analysis results of PPS and RS are shown in Table 1.

The ash content increased to 62.82% for PPS-300–60 and 58.62% for RS-300–60 with the severity of torrefaction as compared to untorrefied PPS and RS. The moisture and the volatile matter contents were reduced to 35.39% and 47.44%, respectively, for PPS-300–60 and 35.01% of moisture, and 20.04% of volatile matter were reduced for RS-300–60 as compared to untorrefied PPS and RS. However, fixed carbon content increased to 64.84% for

PPS-300–60 and 43.87% for RS-300–60 as compared to untorrefied PPS and RS. It may be due to the loss of organic matter during the torrefaction process [24]. Similar results were observed for pigeon pea stalk. The ash content increased to 89.9% for TPS-250–30, 122.8% for TPS-275–30, and the highest ash content obtained 3.8% for TPS-275–45 as compared to raw biomass. An increase in fixed carbon content to 132.4% for TPS-250–30 and 295.4% for TPS-275–30 as compared to raw biomass [28]. Chen et al. reported similar results for rice husk where the volatile matter content decreased from 65.32 to 41.26% and fixed carbon content increased from 18.73 to 35.31%. Whereas ash content increased from 15.95 to 23.43% with

increasing the temperature from 220 to 300 °C under non-oxidative torrefaction of rice husk [14]. Similar results of a decrease in the volatile matter were reported for soybean straw pellets (SSP) and pine wood pellets (PWP) with an increase in torrefaction temperature. Although fixed carbon and ash contents were gradually increased with torrefaction temperature for SSP and PWP [40]. However, the resident time does not affect the proximate analysis, which indicates that temperature plays a significant role in torrefaction than time.

3.2 Effect of torrefaction on combustion indices parameters of PPS and RS

The combustion indices parameters including FR, CI, and VI were derived from the composition of proximate analysis results and heating value of untorrefied and torrefied PPS and RS. The results of FR, CI, and VI are shown in Table 2.

With an increase in torrefaction temperature from 230 to 300 °C with 30 and 60 min of residence time, the fuel ratio (FR) increased from 0.25 to 1.35 for PPS-300–60 and 0.23 to 0.52 for RS-300–60 as compared to untorrefied PPS and RS. Similar results were found with the fuel ratio of pigeon pea stalk (646.2% for TPS-275–45) as compared to RPS [28]. Conag et al. [45] reported that the fuel ratio (0.26 to 1.76) of sugarcane leaves increased with an increase in torrefaction temperature from 250 to 350 °C. FR ratio firmly depends on the volatile matter content of biomass, i.e., if the volatile matter is high, then FR becomes low; it indicates that solid fuel ignites easily due to the presence of high volatile matter and also creates a considerable amount of smoke emission during power generation, and hence, it is problematic to use as solid fuel in power plants [46]. In lower VM content, the results of FR have ignition issues and falling flam stability [47]. In general, the FR ratio varies between 0.5 and 2.0 for coal-fired power plants [45]. However, biomass is generally used in combination with coal, and FR greater than 2.0 creates issues. Hence, moderately torrefied biomass may be considered as solid fuel in combination with coal for power generation. The CI value was gradually decreased to 20.21 MJ/kg for PPS-300–60 as compared to untorrefied PPS (85.27 MJ/kg). For RS, the CI value was 47.09 MJ/kg at 300 °C and 60 min of residence time as compared to untorrefied RS (89.13 MJ/kg). Though, further increasing temperature up to 350 °C with 60 min of residence time, the CI value of RS decreased to 21.23 MJ/kg. It may be due to the release of the volatile contents in RS with the change in temperature and time. The reduced value of the CI for both the torrefied PPS and RS was in good agreement with the reported value [28] for use in power industries as co-combustion with coal. It indicates that the influence of torrefaction temperature certainly improves the compatibility properties of PPS and RS. Singh et al. [28] reported similar

results of CI value for pigeon pea stalk; with an increase in torrefaction temperature, the CI value reduced to 23.3 MJ/kg for TPS-275–45 from 134.9 MJ/kg of RPS. Volatile ignitability (VI) does not follow any regular trend for PPS. The VI value of PPS (17.93 MJ/kg) was reduced to 17.03 MJ/kg with the change in the temperature from 230 to 300 °C with 60 min. The VI value increased to 19.54 MJ/kg from 17.71 MJ/kg for RS with increased temperature and residence time. Similar results of CI and VI were observed by Singh et al. [28] for RPS and Conag et al. [45] for sugarcane leaves. FR ratio, CI, and VI properties passionately depend on VM which was relevant to the torrefaction temperature and time. The VM content in solid fuels reduced and finally converted into fixed carbon when torrefaction temperature and time increased. The differences in volatile ignitability may be due to moisture reabsorption [45].

3.2.1 Effect of torrefaction temperature on higher heating value, mass yield, energy yield, and energy density ratio of PPS and RS

The torrefaction aims to upgrade the higher heating value, energy yield, and energy density ratio of PPS and RS with respect to the change in temperature and time. The heating value increased from 19.50 to 25.29 MJ/kg for PPS and 19.07 to 22.76 MJ/kg for RS with the change in the temperature from 230 to 300 °C and residence time of 30 and 60 min. The HHV increased sharply from 19.94 MJ/kg (PPS-230–60) to 22.25 MJ/kg (PPS-260–30) and 23.72 MJ/kg (PPS-300–30) to 25.29 MJ/kg (PPS-300–60). When increasing the residence time for 30 more minutes during torrefaction at PPS-300–30, the HHV increased to 25.29 MJ/kg for PPS-300–60. The results indicated that time also significantly affected the HHV of PPS. Similar results have been observed that at 300 °C with 8 min of residence time, the HHV obtained was 22.42 MJ/kg. When torrefied for 25 min at 300 °C, the HHV of spruce wood increased to 27.78 MJ/kg. This was due to oxygen and hydrogen contents decreasing during torrefaction while carbon content increased [48]. For RS, HHV increased from 20.35 MJ/kg (RS-260–60) to 22.71 MJ/kg (RS-300–30). Further increasing the time for 30 more minutes at RS-300–30, the HHV increased to 22.76 MJ/kg for RS-300–60. When increasing the temperature and time up to 350 °C and 60 min of residence time, the HHV increased to 24.30 MJ/kg for RS. It was comparable with the HHV of coal (24 MJ/kg) for heat and power generation applications [49]. The results showed that the heating value was significantly affected by torrefaction temperature and time for PPS and RS. The changes in the heating value of PPS and RS with respect to changes in temperature and time were shown in Fig. 3. The increment of HHV of PPS and RS was due to the increased carbon content by the loss of oxygen- and hydrogen-containing

volatile compounds during torrefaction. Similar results were reported for pigeon pea stalk: the HHV increased from 16.67 to 21.43 MJ/kg when torrefied from 225 to 275 °C with a residence time of 45 min [28]. Chen et al. stated that the HHV of rice husk increased from 16.79 MJ/kg for RH raw to 18.91 MJ/kg for RH-300–0 [14] during non-oxidative torrefaction. We found similar results in another report where the HHV increased to 21.1 MJ/kg for SSP-350 and 24.0 MJ/kg for PWP when torrefied from 200 to 350 °C [40]. The results suggested that torrefaction improves the quality of the biomass.

Changes in mass yield and energy yield of torrefied PPS and RS with temperature and time were also studied. For PPS, the energy yield was decreased gradually from 78.49% for PPS-230–30 to 71.41% for PPS-260–60. When increasing torrefaction and time, the mass yield was decreased sharply from 66.88% for PPS-300–30 to 58.35% for PPS-300–60 as compared to the untorrefied PPS. Similarly, for RS, the energy yield was decreased gradually from 89.18% for RS-230–30 to 80.00% for RS-300–30. While increasing temperature up to 300 °C with 60 min of residence time, the energy yield decreased sharply to 71.61% for RS-300–60. Mass yields also decreased from 77.00% for PPS-230–30 to 60.00% for PPS-260–60. At 300 °C, the yield was decreased sharply from 55.00% for PPS-300–30 to 45.00% for PPS-300–60 as compared to untorrefied PPS. Similarly, for RS, the mass yield was decreased from 87.42% for RS-230–30 to 77.00% for RS-260–60. When torrefied at 300 °C with 30 and 60 min of residence time, the mass yield was decreased from 67.00% for RS-300–30 to 60.00% for RS-300–60 as compared to untorrefied RS. Up to 260 °C, the mass yield decreased gradually, whereas the torrefaction duration time did not affect the yield. At 300 °C, the residence time had
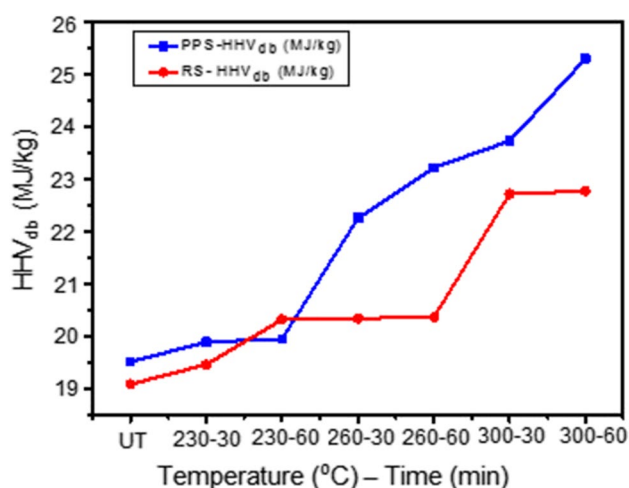

Fig. 3 HHV of untorrefied and torrefied PPS and RS with the change in the temperature from 230 to 300 °C with residence time of 30 and 60 min

significantly affected the torrefaction of PPS and RS due to the intensive decomposition of cellulose [44]. The energy yield mainly depends on the mass yield of the torrefied PPS and RS. With an increase in torrefaction temperature, the mass yield decreased due to the loss of volatile matter and degradation of hemicellulose and cellulose. Chen et al. also reported similar results for both mass and energy yield in oxidative and non-oxidative torrefaction of rice husk from 220 to 300 °C. In another study, Chen et al. reported similar results; the mass yield of SSP-350 and PWP-350 was less than 45%. However, the energy yield was obtained to 57.8% for SSP-350 and 68.9% for PWP-350. This was due to the increasing enhancement factor of torrefied pellets [40]. Singh et al. [28] reported similar results for pigeon pea stalk; as increased the torrefaction temperature from 225 to 275 °C, the energy yield decreased from 0.84 to 0.50 for pigeon pea stalk. In this study, the fuel quality of PPS and RS has been improved with the severity of torrefaction temperature.

The energy density ratio was derived from the higher heating value of torrefied PPS and RS and the lower value of untorrefied PPS and RS. The energy density ratio increased to 1.19 MJ/kg for RS-300–60 and 1.30 MJ/kg for PPS-300–60 as compared to untorrefied RS and PPS. The energy density ratio increased sharply from 19.67% (PPS-300–30) to 27.73% (PPS-300–60) and 17.06% (RS-300–30) to 17.33% (RS-300–60). The variations in the energy density ratio of PPS and RS are due to differences in the heating values with respect to the loss of volatile matter and moisture content during the torrefaction process. Similar results have been observed for pigeon pea stalk that the energy density increased from 2826.9 MJ/kg for TPS-250–15 to 2863.4 MJ/m^3 for TPS-250–30 and 2828.2 MJ/kg (TPS-275–15) to 2844 MJ/m^3, as compared to 2705.5 MJ/m^3 for RPS. It indicated that the torrefaction had little or no effect on energy density above 250 °C [28]. Conag et al. [45] reported that the energy density ratio increased from 1.0 for raw SCL to 1.38 for SCL-300–75 and suggested that the high energy density ratio is not required to be an absolute measure of torrefaction performance. The energy density ratio of PPS and RS is increased by torrefaction and becomes good quality solid biofuel for other courses such as pyrolysis and gasification [50].

3.3 Effect of torrefaction on the functional groups of PPS and RS agro-waste

FTIR spectroscopy has been used to study the changes in functional groups of PPS and RS at various torrefaction temperatures and residence time (Fig. 4a, b).

The details of the changes in wave number and intensity of functional groups of PPS are shown in Supplementary information in Table S2. FTIR absorbance bands of

Fig. 4 Infrared spectra of **a** untorrefied and torrefied agrowaste of PPS with the change in temperature from 230 to 300 °C with the residence time of 30 and 60 min **b** assigned part of IR spectra from 1800 to 1000 cm^{-1}
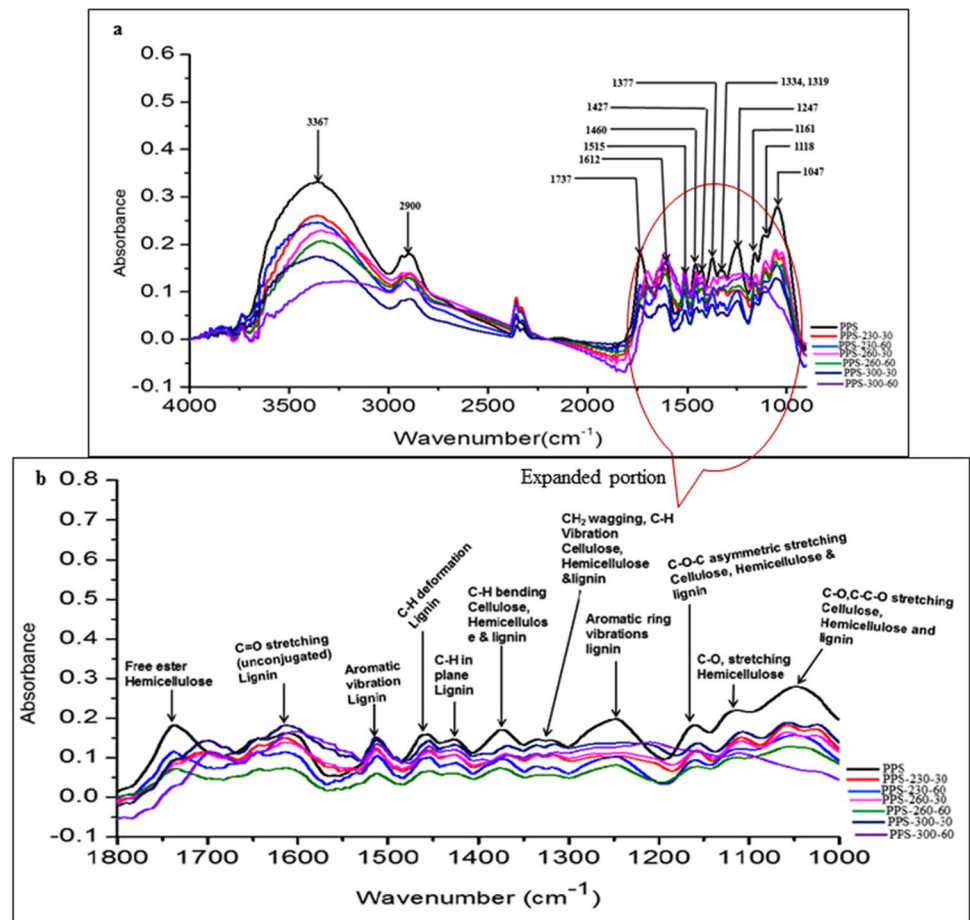

untorrefied and torrefied PPS and RS were assigned from the literatures [51–54]. The intensity of the O–H band reduced with an increase in torrefaction temperature and time. It may be attributed due to dehydration and degradation of the –OH band in hemicellulose and cellulose [55]; as a result, the O–H band becomes broad. Moreover, the O–H band was shifted from 3367 to 3224 cm^{-1}. Similar results have been reported for torrefied bamboo, SSP, and PWP [13, 40]. The bands at about 2900 cm^{-1} for PPS and 2906 cm^{-1} for RS were observed for C–H aliphatic symmetrical band due to the presence of methyl and methylene groups in alkane and alkene; when temperature increased from 230 to 300 °C with residence time of 30 and 60 min, the C–H aliphatic symmetrical band shifted to 2914 cm^{-1} for PPS-300–60 and 2915 cm^{-1} for RS-300–60 due to degradation of methyl and methylene groups in alkane and alkene. Singh et al. [28] reported similar results that the C–H aliphatic symmetrical band shifted from 2892 to 2908 cm^{-1} in pigeon pea stalk due to removal of methyl and methylene groups in alkane and alkene with increasing torrefaction temperature. The band appeared at about 1737 cm^{-1} for vibrational stretching of C=O when torrefied from 230 to 300 °C with 30 and 60 min; the C=O group diminished and reappeared

at a lower wavelength of 1693 cm^{-1} [13]. Chen et al. [40] reported that the peak appeared at 1700 cm^{-1} for C=O in the stretching and the bending vibration of acetyl groups in hemicellulose; when torrefied at 350 °C, the peak disappeared due to decomposition of the polymeric structure of SSP and PWP at high temperature. The conjugated C=C stretching vibrations in the aromatic ring of lignin band appeared at 1515 cm^{-1} for untorrefied PPS, and 1595 cm^{-1} for untorrefied RS was decomposed when torrefied at 300 °C with 60 min of residence time, and the band appeared at a lower wave number at about 1509 cm^{-1} for PPS and higher wave number about 1612 cm^{-1} for RS. The C–H deformation band in the lignin appeared at 1460 cm^{-1} for PPS and 1462 cm^{-1} for RS. At 300 °C, the C–H bands appeared at 1452 cm^{-1} for PPS and 1509 cm^{-1} for RS due to lignin degradation. The C–O–C stretching vibrations in cellulose and hemicellulose appeared about 1161 cm^{-1} for PPS and RS; when torrefied at 230 °C with 60 min of residence time, this band shifted to a lower wave number about 1157 cm^{-1} for PPS and 1159 cm^{-1} for RS. With an increase in torrefaction temperature up to 300 °C, the band of C–O–C stretching vibrations in cellulose and hemicellulose appeared at 1209 cm^{-1} for PPS and 1157 cm^{-1} for RS. It indicates that

the hemicellulose and cellulose undergo partial thermal decomposition from 230 to 300 °C with 30 and 60 min of residence time and hemicellulose being more significantly affected [28]. The C–O– stretching vibrations in cellulose appeared at about 1118 cm^{-1} for PPS and 1109 cm^{-1} for RS; when temperature increased to 300 °C, this band was shifted to 1105 cm^{-1} for PPS and 1112 cm^{-1} for RS. The C–O– band slightly shifted to a higher wave number for RS at the higher temperature may be due to partial degradation of the polymeric structure. The C–C–O stretching vibrations of alcoholic groups in cellulose appeared about 1047 cm^{-1} for PPS and 1053 cm^{-1} for RS with the torrefied temperature at 300 °C with the residence time of 30 and 60 min; the bands were shifted to 1024 cm^{-1} for PPS, and the C–C–O band remains unchanged for RS at 1053 cm^{-1}. However, the intensity of the band was decreased with the torrefaction. Some of the functional groups of PPS and RS were shifted to the higher wave number with the change in temperature and time. It could be due to the oxygen-containing functional groups of the organic molecules being gradually removed. As a result, the intensity of the band diminished

with the severity of torrefaction temperature. The peaks of SSP and PWP in the range of 1500–1100 cm^{-1} correspond to the spectra of stretching bending peaks of C–O–C, C–H, and C–OH and were not changed at 200–250 °C. However, when torrefaction increased from 300 to 350 °C, the bonds of C–O–C, C–H, and C–OH are broken and produce ketones and furans [40]. The changes in intensity and wave number of functional groups of RS are shown in Fig. 5a, b. Due to the severity of torrefaction, the volatile components of the polymeric structure of organic molecules were progressively degraded; thus, the intensity of the band diminished. The details of the changes in the wave number and intensity of functional groups of RS are shown in Supplementary information in Table S3. The broadening of the O–H band in IR spectra may be due to intermolecular and intramolecular hydrogen bonding in crystalline hemicellulose and cellulose compounds. The variation in the intensity and wave number of functional groups in PPS and RS was probably due to the prior decomposition of polysaccharides in PPS than RS with increased torrefaction temperature; thus, PPS and RS become more hydrophobic.

Fig. 5 Infrared spectra of **a** untorrefied and torrefied agro-wastes of RS with the change in temperature from 230 to 300 °C with the residence time of 30 and 60 min **b** assigned part of IR spectra from 1800 to 1000 cm^{-1}
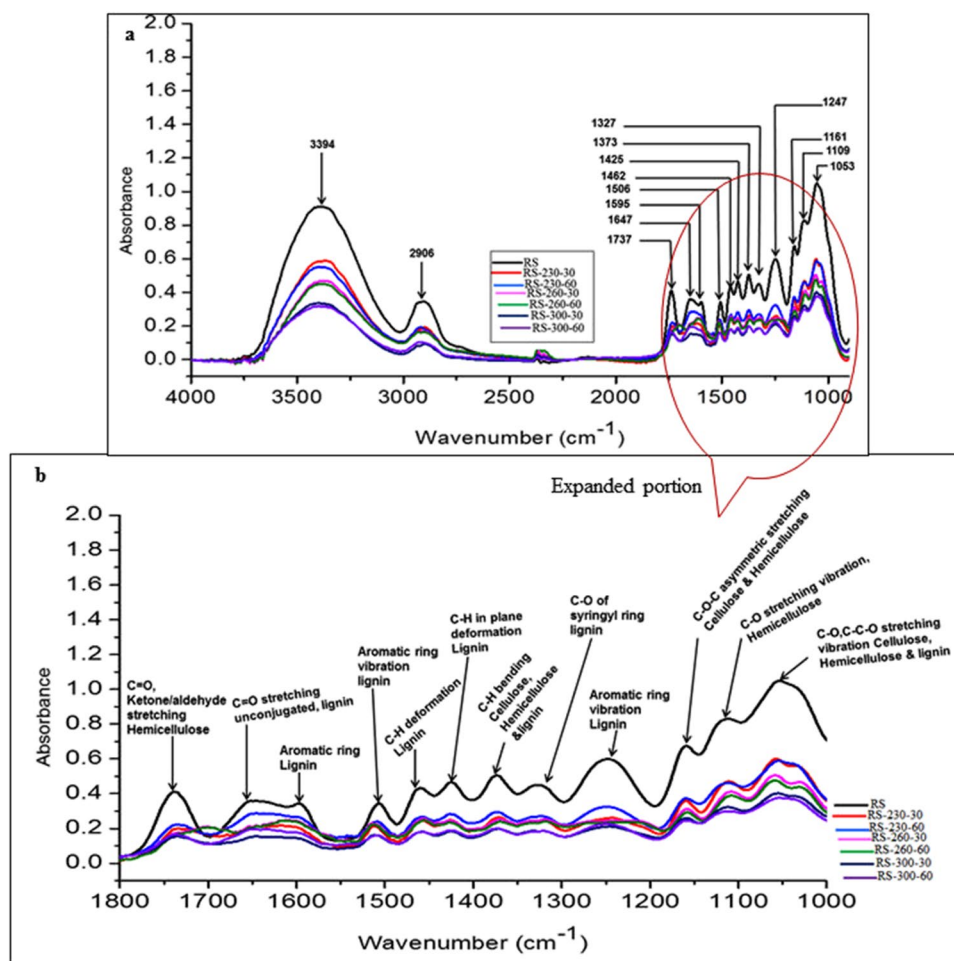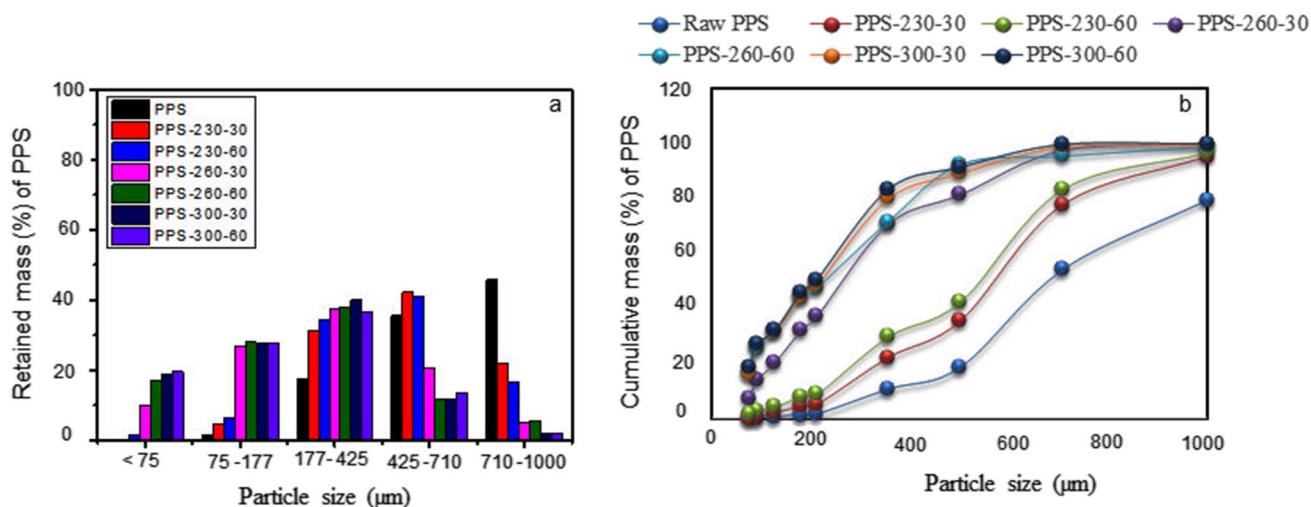
Fig. 6 Particle size distribution (**a**) retained mass weight (%). **b** Cumulative particle size distribution of PPS after grinding
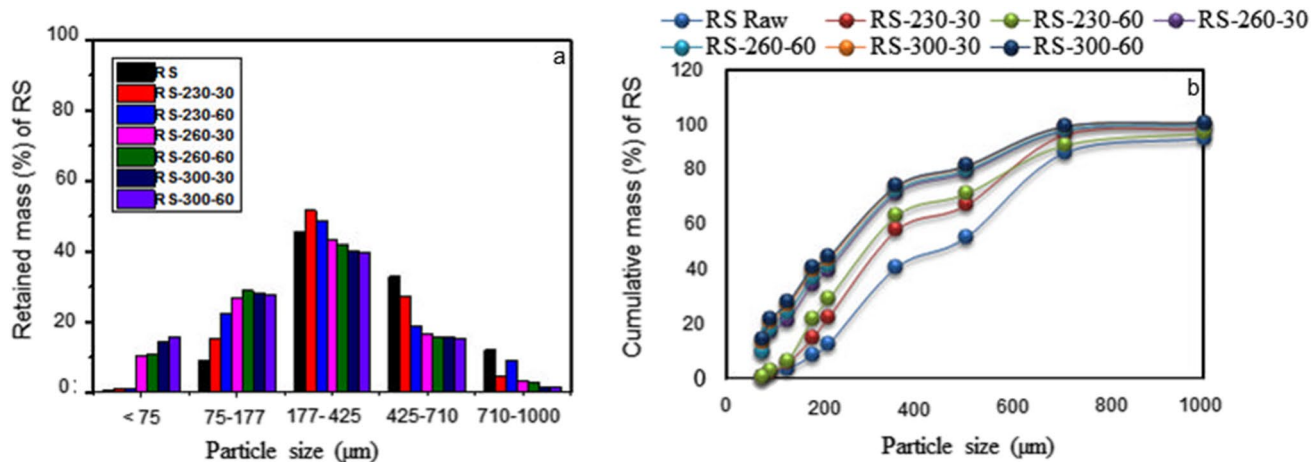

Fig. 7 Particle size distribution (**a**) retained mass weight (%). **b** Cumulative particle size distribution of RS after grinding

3.4 Effect of torrefaction on grindability of PPS and RS

To get detailed information about the grinding behavior of PPS and RS with the change in temperature and time, we followed the particle size distribution [27, 55] method. After grinding, the ground particles of PPS and RS were separated with five different sizes of sieves, including < 75, 75–177, 177–425, 425–710, and 710–1000 μm (s) by using a sieve shaker. The retained mass percentage of PPS and RS with the change in the temperature and time are shown in Figs. 6 and 7.

Some difficulties were found in the result during the size reduction of the PPS and RS due to the fibrous nature of hemicellulose and cellulose component linkages; the results are shown in Figs. 6a and 7a.

About 0.02% and 0.74% of ground particles of untorrefied PPS and RS, respectively, were passed through a < 75-μm sieve size. However, when the PPS and RS were torrefied, the ground particles of about 19.71% for PPS-300–60 and 15.68% for RS-300–60 were passed through a < 75-μm sieve as compared to untorrefied PPS and RS. A higher fraction of smaller particles was found on 177–425-μm sieve for both the PPS and RS residue(s) after distributing particles between five different sieve sizes. It may be due to the re-absorption of moisture during the grinding process. However, the grindability of PPS and RS was improved by the loss of fibrous nature of PPS and RS when torrefaction temperature increased; as a result, the PPS and RS become more brittle and easy to grind. The comparison of grindability of PPS and RS at 300 °C with 30 and 60 min of residence time is shown in Fig. 8.
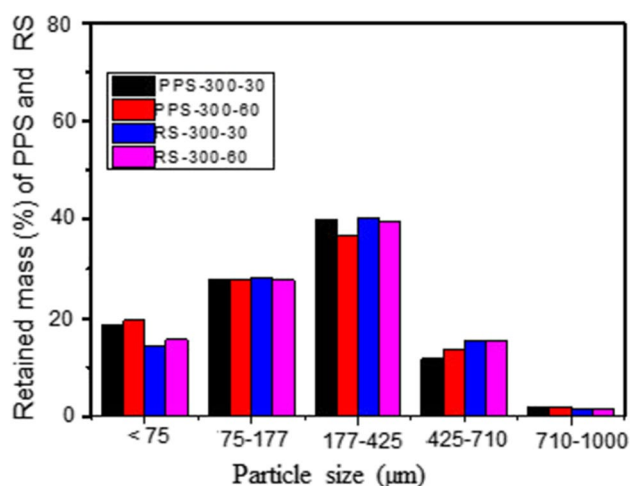
Fig. 8 Comparison of grindability behavior of PPS and RS at 300 °C with the residence time of 30 and 60 min

About 99.89% of the smallest particles were passed through a < 75-μm sieve for PPS and 95.28% for RS when torrefied at 300 °C and 60 min of residence time as compared to untorrefied PPS and RS. This happened because of the decomposition of the polymeric nature of cellulose, hemicellulose, and lignin at 300 °C for 60 min. Cumulative particle size distribution curves of ground torrefied PPS and RS were shifted towards smaller fractions. Comparatively, the PPS has a higher (19.71%) proportion of smaller particles obtained than the RS (15.68%) at 300 °C temperature and 60 min of residence time. The variation in the distribution of smaller particles between the torrefied PPS and RS may be due to prior degradation of organic matter in PPS and the presence of extra moisture in RS. Up to 260 °C, the fraction of smaller ground particles had been increased gradually, and residence time has no effect. At 300 °C, the fraction of smaller ground particles increased sharply, and the duration of time (residence time) had significantly affected

the grindability of torrefied PPS and RS due to the intensive decomposition of cellulose. Bridgeman et al. [56] reported the torrefaction temperature as an essential factor in biomass (energy crop) grinding to smaller sizes. However, residence time also significantly affected the grindability to produce a smaller fraction of particles.

Nevertheless, after torrefaction, the torrefied PPS which produced the highest percentage of smaller particles can be considered as best grindability [27]. Similar results were observed by Tapasvi et al. [25] with an increase in the percentage of fine particles when torrefied; the Norwegian birch and spruce decreased the average particle sizes of torrefied biomass [24]. The grinding behavior of PPS and RS has similar fashions with other torrefied biomasses such as Norwegian birch, spruce, pine, black poplar, and chestnut [24, 25] that are used as a blend with coal for co-firing. Hence, the torrefied PPS and RS may be useful for co-firing with coal.

3.5 Effect of torrefaction on mechanical properties of the pellets of PPS and RS

The physical appearance of PPS and RS pellets was changed to darker and rough with increased temperature from 230 to 300 °C and the residence time of 30 and 60 min. It may be due to the breakage of the polymer's chemical structure in lignin [31, 57, 58] than the untorrefied pellets. The physical appearances of untorrefied and torrefied PPS and RS pellets were shown in Fig. 9.

Mechanical properties of the PPS and RS pellets were studied with reference to the crushing strength and durability tests.

3.5.1 Effect of torrefaction on crushing strength or hardness and durability of PPS and RS pellets

The crushing strength and durability of untorrefied and torrefied PPS and RS pellets are shown in Supplementary

Fig. 9 Physical appearance of untorrefied and torrefied PPS and RS pellets with the change in temperature and time

information in Table S4. Crushing strength was investigated by applying load gradually on the pellets until it fractures or breaks. The pellet crushing strength was observed to be 55 kg for PPS (untorrefied) and 45 kg for RS (untorrefied). The crushing strength decreased from 55 kg (PPS) to 50 kg, 48 kg, 10 kg, 8 kg 2 kg, and 1 kg for PPS-230–30, PPS-230–60, PPS-260–30, PPS-260–60, PPS-300–30, and PPS-300–60, respectively, as compared to untorrefied PPS pellets. The crushing strength decreased sharply to 1 kg for PPS at 300 °C and residence time of 60 min as compared to untorrefied PPS. Unlike the PPS, the crushing strength for RS pellets decreased gradually from 45 kg (RS) to 40 kg, 38 kg, 35 kg, 30 kg, 28 kg, and 20 kg for RS-230–30, RS-230–60, RS-260–30, RS-260–60, RS-300–30, and RS-300–60, respectively, as compared to untorrefied RS pellets. When the temperature increased, the bonding between the particles reduced within the pellet matrix. The pellets become brittle by the loss of the polymeric nature of the chemical structure [39]. As a result, PPS pellets become nonpolar, and the gaps between the particles within the pellet matrix increased [59]. Subsequently, crushing strength became negligible for PPS-300–60. The dissimilarity of crushing strength between the pellets of PPS and RS may be due to the hydrogen bonding that may play a crucial role in the extra moisture content of torrefied RS pellets. Shang et al. reported similar results that the crushing strength of wood pellets reduced to 90% at 260 °C and 60 min of residence time; as a result, the pellets became brittle and lower in hardness and finally difficult to handle, store, and transport [31]. The crushing strength of the untorrefied and torrefied pellets increased with increasing the compaction pressure from 5.50 to 10.30 tonnage of pressure. It was due to the formation of interparticle bonding such as
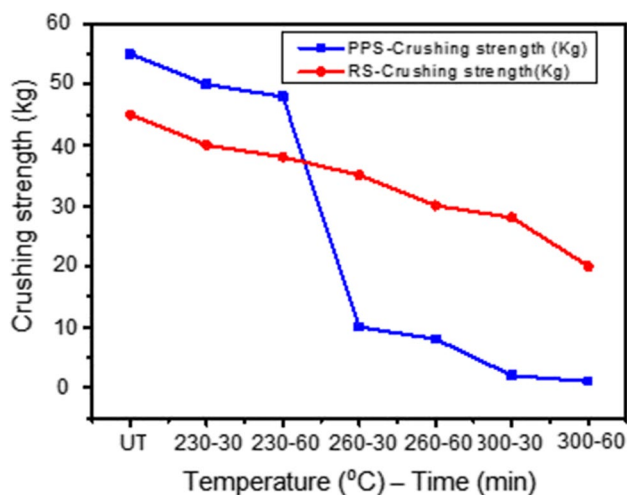
intermolecular hydrogen bonding, van der Waals' forces, and electrostatic force of interactions between particles of starch, protein, lignin, and water-soluble carbohydrate, and those are encouraged to form solid bridges in pellet matrix [60]. It was observed that the crushing strength of untorrefied PPS and RS pellets was higher than torrefied pellets; this was due to the presence of H-bonding and van der Waals force of interactions in addition to mechanical interlocking in the particles of the pellet matrix [39]. The crushing strength of pellets of PPS and RS is shown in Fig. 10.

3.5.2 Effect of torrefaction on the durability of PPS and RS pellets

The durability of the untorrefied and torrefied pellets of PPS and RS is shown in Fig. 11.

In general, torrefied pellets have lower durability than untorrefied pellets [61]. The durability of untorrefied PPS and RS pellets was 97.68% and 94.51%, respectively, at 10.30 tonnage pressure.

The durability of PPS and RS pellets decreased with increased torrefaction temperature and residence time at the compaction pressure of about 10.30 tonnages. The durability of PPS pellets decreased sharply from 95.52% (PPS-230–60) to 37.53% (PPS-300–60) as compared to untorrefied PPS pellets at 10.30 tonnage of compacting pressure. In contrast to the PPS pellets, the durability of RS pellets was decreased at a slower rate from 93.61% (RS-230–30) to 84.29% (RS-300–60) at the same compacting pressure as compared to untorrefied RS pellets. This is due to the thermal decomposition of biomass when the severity of torrefaction temperature increased; as a result, the pellets became less dense, and subsequently, the durability decreased. When the torrefaction
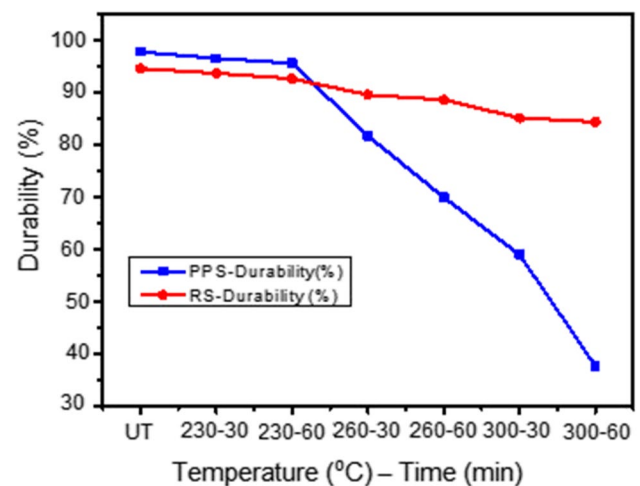

Fig. 10 Crushing strength of PPS and RS pellets with the change in temperature and time

Fig. 11 Durability of PPS and RS pellets with the change in the temperature from 230 to 300 °C and the residence time of 30 and 60 min

temperature increased, the lignin became soft and acted as a natural binder within the pellet matrix. Consequently, it became hard and improved the nonpolar C–C bonds while reducing the hydroxyl groups in lignin [61]. On the other hand, RS particles in the pellet matrix become hard. It is difficult to form bonding within the particles of the torrefied pellet matrix [62]. It was perceived that the durability differences between the pellets of PPS and RS might be due to the loss of volatile matter, moisture, destruction of cell walls, and prior decomposition of organic molecules present in the pellet matrix of PPS [28]. As a result, PPS and RS became more brittle and weaker in tenacious structures, and mechanical properties become poor. As the compaction pressure increased from 5.50 to 10.30 tonnages, the durability of PPS and RS pellets [63] increased. This is probably due to the formation of molecular bonding between the particles within the pellet matrix [64]. The details of the results are shown in Supplementary information in Table S4. A similar result was reported that the durability decreased by 36.8% for SSP-350 and 21.3% for PWP-350 as compared to raw SSP (99.32%) and PWP (99.46%). This was mainly due to the increased torrefaction temperature, thermal decomposition of biomass, and the torrefied pellets becoming less dense. Subsequently, the factor lowers the mechanical properties. It was suggested that torrefaction should be adopted at 250 °C for SSP and 300 °C for PWP [40]. Ghiasi et al. [37] prepared the torrefied pellets by two different process routes, i.e., first pellets were prepared followed by torrefaction (scheme-I) or first done torrefaction followed by the pelletization (scheme-II) to convert Douglas-fir wood chips to torrefied wood pellets. Scheme-II pellets have higher durability (98.6%) than scheme-I pellets (97.0%).

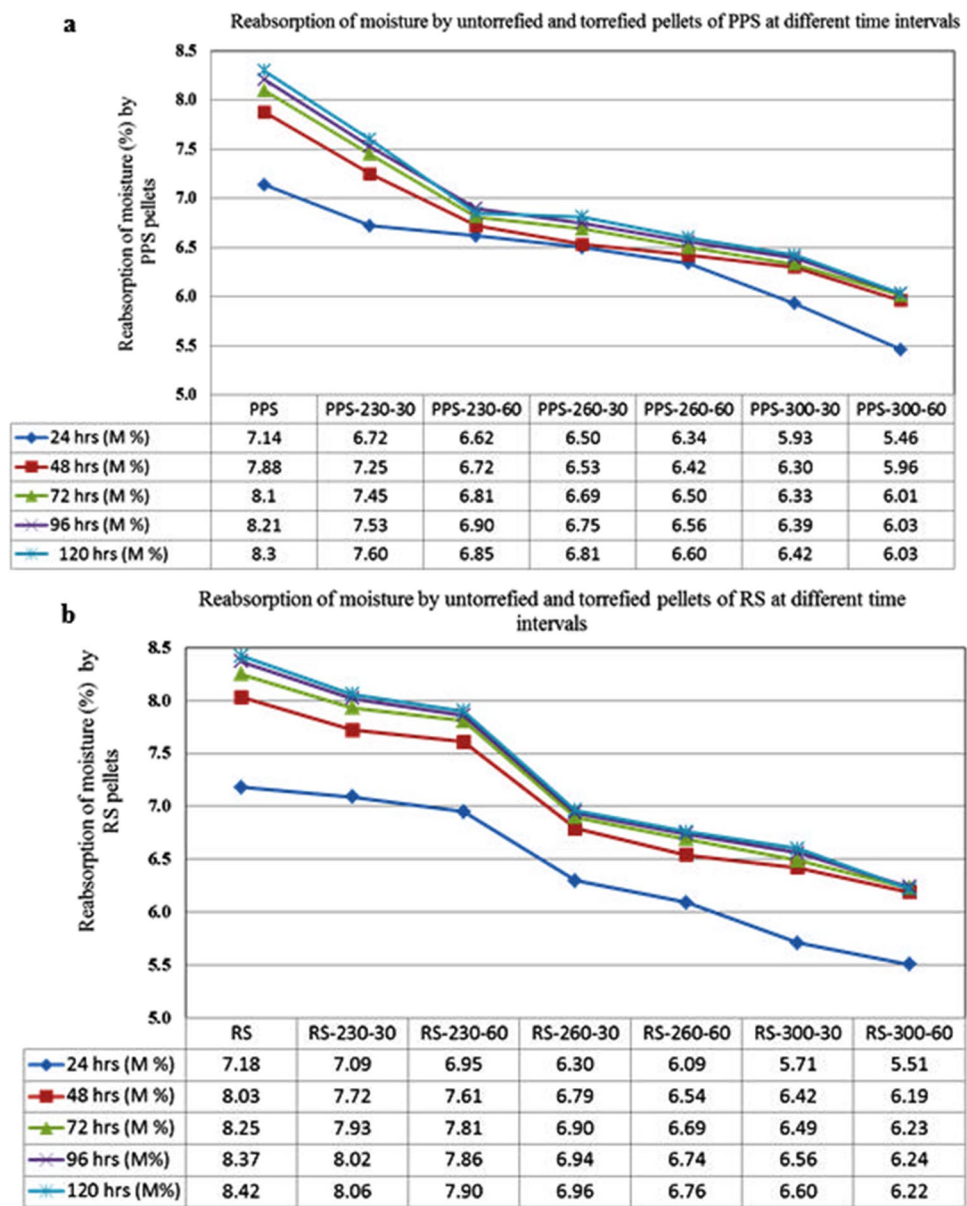## 3.6 Effect of torrefaction on moisture reabsorption tendency (equilibrium moisture content)

Moisture reabsorption tendency of PPS and RS was determined for untorrefied and torrefied pellets. It was observed that the untorrefied PPS and RS pellets have more affinity towards the reabsorption of moisture than torrefied PPS and RS pellets when exposed to controlled environment condition of 60% relative humidity (RH) at 40 °C temperature for 120 h. We found a similar trend for the reabsorption of moisture by both PPS and RS pellets with increasing torrefied temperature and time. With an increase in torrefaction temperature, the moisture reabsorption tendency decreased from 7.14% for PPS to 5.46% for PPS-300–60 and 7.18% for RS to 5.51% for RS-300–60 at 24 h. When PPS and RS pellets were kept for 120 h in 60% RH at 40 °C, the reabsorption of moisture tendency decreased. The moisture levels of the PPS and RS at different time intervals are as the following: 23.36% for PPS-300–60 and 22.91% for RS-300–60 after 48 h, 25.80% for PPS-300–60 and

24.48% for RS-300–60 after 72 h, 26.55% for PPS-300–60 and 24.48% for RS-300–60 after 96 h, and 27.35% for PPS-300–60 and 26.12% for RS-300–60 after 120 h. The results of the moisture reabsorption tendency are shown in Fig. 12. The moisture reabsorption tendency decreased due to the loss of hydroxyl and acid groups in the polymeric structure when torrefaction temperature increased. The untorrefied pellets of PPS have less affinity to the reabsorption of moisture than the untorrefied RS pellet due to the availability of hydroxyl and acid groups in hemicellulose, cellulose, and lignin [65, 66]. With an increase in torrefaction temperature, there was a loss of hydrogen, oxygen, acids, esters, and other hydrophilic groups in the polymer matrix of pellets. As a result, pellets can be effortlessly resistant to moisture reabsorption and have a greater potential for storage and transportation [41]. Chen et al. [40] reported similar results that the equilibrium moisture content of SSP-350 and PWP-350 decreased to 50% for SSP-350 and 70% for PWP-350 as compared to raw SSP (9.5%) and PWP (9.7%). Singh et al. [28] reported that with an increase in torrefaction temperature, the reabsorption of moisture of pigeon pea stalk decreased from 6.31 to 7.65% for TPS-225–30 to 3.97 to 4.98% for TPS-275–30 after 96 h as compared to moisture reabsorbed after 48 h. With an increase in time intervals, the moisture reabsorption tendency of PPS-300–60 and RS-300–60 decreased gradually as compared to untorrefied pellets of PPS and RS pellets. The decrease in the moisture reabsorption of PPS and RS pellets has a great advantage for the storage and transportation of biomass pellets. The reabsorption of moisture by untorrefied and torrefied PPS and RS pellets at 60% RH at 40 °C with different time intervals is shown in Fig. 12.

3.7 Industrial quality parameters of PPS and RS pellets

Combustion indices parameter such as fuel ratio (FR) was 1.35 for PPS-300–60 and 0.52 for RS-300–60. FR ratio of torrefied PPS and RS was similar to the reported results for blending with coal in power industries [40, 67, 68]. The CI value was 20.21 MJ/kg for PPS-300–60 and 47.09 MJ/kg for RS-300–60. However, with an increase in torrefaction temperature up to 350 °C and 60 min for RS, the CI value increased to 21.23 MJ/kg. Therefore, the CI values of both PPS and RS are similar to the reported results of coal used in power industries [62]. Moisture contents reduced to 4.80%, and ash content increased to 1.91% for PPS; and the respective reduction for RS was 4.90% and 2.61%. The durability of untorrefied PPS and RS pellets was 97.68% and 94.51% which is comparable with Industrial Quality and EN-plus Quality [69, 70] of industrial wood pellets. The results of PPS and RS are compared with previous studies as shown in Table 3.

Fig. 12 Reabsorption of moisture by untorrefied and torrefied **a** PPS and **b** RS pellets at 60% RH at 40 °C with different time intervals

a Reabsorption of moisture by untorrefied and torrefied pellets of PPS at different time intervals

	PPS	PPS-230-30	PPS-230-60	PPS-260-30	PPS-260-60	PPS-300-30	PPS-300-60
24 hrs (M %)	7.14	6.72	6.62	6.50	6.34	5.93	5.46
48 hrs (M %)	7.88	7.25	6.72	6.53	6.42	6.30	5.96
72 hrs (M %)	8.1	7.45	6.81	6.69	6.50	6.33	6.01
96 hrs (M %)	8.21	7.53	6.90	6.75	6.56	6.39	6.03
120 hrs (M %)	8.3	7.60	6.85	6.81	6.60	6.42	6.03

b Reabsorption of moisture by untorrefied and torrefied pellets of RS at different time intervals

	RS	RS-230-30	RS-230-60	RS-260-30	RS-260-60	RS-300-30	RS-300-60
24 hrs (M %)	7.18	7.09	6.95	6.30	6.09	5.71	5.51
48 hrs (M %)	8.03	7.72	7.61	6.79	6.54	6.42	6.19
72 hrs (M %)	8.25	7.93	7.81	6.90	6.69	6.49	6.23
96 hrs (M%)	8.37	8.02	7.86	6.94	6.74	6.56	6.24
120 hrs (M%)	8.42	8.06	7.90	6.96	6.76	6.60	6.22

4 Conclusions

The impact of torrefaction on physicochemical properties, grindability, moisture reabsorption tendency, and mechanical properties of binderless pellets/agro-waste of PPS and RS was evaluated in this work. Fuel quality of PPS and RS improved with an increase in torrefaction temperature. Fuel ratio and CI values of PPS and RS increased with an increase in torrefaction temperature from 230 to 300 °C and residence time from 30 to 60 min. Fixed carbon and HHV of torrefied PPS and RS increased by the loss of oxygen and hydrogen, chloride, ester, and other organic groups in polymeric organic structure. The grindability of PPS and RS improved and confirmed by the passes of ground particles of about 99.89% for PPS-300–60 and

95.28% for RS-300–60 through < 75-μm sieve size as compared to untorrefied PPS and RS. The changes in the intensity and wave number of PPS and RS functional groups were confirmed by reducing the band intensity and wave number shift, for example, -OH (3367–3224 cm^{-1}), ester groups (1737–1693 cm^{-1}), –C–O–C– (1161–1209 cm^{-1}), and –C–C–O– alcoholic groups (1047–1024 cm^{-1}). The mechanical properties of PPS and RS pellets were assessed in terms of crushing strength and durability. The crushing strength decreased from 55 to 1 kg for PPS-300–60 and 45 to 20 kg for RS-300–60. The durability decreased from 96.45% (PPS-230–30) to 37.53% (PPS-300–60) and 93.61% (RS-230–30) to 84.29% (RS-300–60). The results indicated that the torrefaction may be suitable up to 260 °C for PPS and 300 °C for RS with respect to the

Table 3 Comparison of ash, volatile matter, FC, energy density, and heating value of PPS and RS with other residues on air-dried basis

Untorrefied/torrefied agro-wastes	Ash (%)	Volatile matter (%)	FC (%)	Energy density	HHV (MJ/kg)	Researchers
PPS	0.66	73.59	18.32	—-	18.05	Present study
PPS-230–30	0.96	71.21	21.08	1.02	18.54	
PPS-230–60	0.98	69.23	23.29	1.02	18.64	
PPS-260–30	1.26	61.99	31.14	1.14	21.01	
PPS-260–60	1.32	59.59	33.70	1.19	21.96	
PPS-300–30	1.73	53.16	40.17	1.22	22.55	
PPS-300–60	1.82	39.78	53.60	1.30	24.07	
RS	1.00	74.23	17.23	—-	17.63	
RS-230–30	1.19	74.19	17.43	1.02	18.05	
RS-230–60	1.26	71.08	21.06	1.07	18.97	
RS-260–30	1.40	70.82	21.91	1.07	19.04	
RS-260–60	1.60	70.56	22.27	1.07	19.22	
RS-300–30	2.24	62.05	30.72	1.19	21.57	
RS-300–60	2.48	61.04	31.58	1.19	21.64	
Rape stalk	3.16	76.35	19.30	NA	18.75	Deng et al. [71]
Rape stalk-200–30	NA	NA	NA	NA	19.50	
Rape stalk-250–30	NA	NA	NA	NA	21.10	
Rape stalk-300–30	NA	NA	NA	NA	21.59	
Cotton stalk	6.53	75.38	18.09	NA	16.53	Chen et al. [72]
Cotton stalk-220–30	7.19	74.25	18.56	NA	17.09	
Cotton stalk-250–30	9.92	69.76	20.32	NA	18.85	
Cotton stalk-280–30	11.28	56.23	32.49	NA	20.31	
Palm kernel shell	4. 38	83.38	10.50	NA	18.16	Onyeagba, Obinna et al. [73]
Palm kernel shell-240–120	8. 40	63.56	28.25	NA	21.54	
Palm kernel shell-260–120	6. 09	70.84	22.72	NA	20.91	
Palm kernel shell-280–120	8. 39	58.07	32.86	NA	21.86	
Palm kernel shell-300–120	10.69	45.30	43.00	NA	22.80	
Coconut shell	1.10	79.56	19.34	NA	19.58	Tanchuling et al. [74]
Coconut shell-250–30	1.52	73.80	24.68	NA	21.58	
Coconut shell-250–60	1.90	63.55	34.55	NA	23.75	
Coconut shell-300–30	1.80	45.78	52.42	NA	27.68	
Coconut shell-300–60	1.81	48.68	49.50	NA	27.24	

mechanical properties. The moisture reabsorption tendency decreased to 27.35% for PPS-300–60 and 26.13% for RS-300–60 at 120 h as compared to untorrefied PPS and RS pellets. The results indicated that the reabsorption of moisture tendency decreased due to torrefaction. The hydrophobic nature of the PPS and RS pellets is encouraging for storage and transportation. The FTIR studies of PPS and RS strongly support the decrease in moisture reabsorption tendency of PPS and RS pellets. Overall, torrefaction of palmyra, redgram, and other similar residues improves the fuel value and convenience of practical handling and storage.

Declarations

Conflict of interest The authors declare no competing interests.

References

1. NPMCR. Available online: http://agricoop.nic.in/sites/default/files/NPMCR_1.pdf. Accessed on 6 March 2019

2. Patel M, Zhang X, Kumar A (2016) Techno-economic and life cycle assessment on lignocellulosic biomass thermochemical conversion technologies: a review. Renew Sustain Energy Rev 53:1486–1499. https://doi.org/10.1016/j.rser.2015.09.070

3. Ullah K, Sharma VK, Dhingra S, Braccio G, Ahmad M, Sofia S (2015) Assessing the lignocellulosic biomass resources potential in developing countries: a critical review. Renew Sustain Energy Rev 51:682–698. https://doi.org/10.1016/j.rser.2015.12.322

4. Cai J, He Y, Yu X, Banks SW, Yang Y, Zhang X (2017) Review of physicochemical properties and analytical characterization of lignocellulosic biomass. Renew Sustain Energy Rev 76:309–322. https://doi.org/10.1016/j.rser.2017.03.072

5. Alexis SG, Cabello Eras JJ, Luc H, Carlo V (2017) The biomass based electricity generation potential of the Province of Cienfuegos Cuba. Waste Biomass Valori 8:2075–2085. https://doi.org/10.1007/s12649-016-9687-x

6. Elsayed M, Chuan W, Johan R, Mikael L (2016) Biomass applications in iron and steel industry: an overview of challenges and opportunities. Renew Sustain Energy Rev 65:1247–1266. https://doi.org/10.1016/j.rser.2016.07.061

7. Loan TT, Vo PN (2016) Treatments of plant biomass for cementitious building materials – a review. Construct Build Mater 121:161–176. https://doi.org/10.1016/j.conbuildmat.2016.05.125

8. Chen DY, Wang Y, Liu YX, Cen KH, Cao XB, Ma ZQ (2019) Comparative study on the pyrolysis behaviors of rice straw under different washing pre-treatments of water, acid solution, and aqueous phase bio-oil by using TG-FTIR and Py-GC/MS. Fuel 252:1–9. https://doi.org/10.1016/j.fuel.2019.04.086

9. Li K, Wang Z-x, Zhang G, Cui M-s, Lu Q, Yang Y (2020) Selective production of monocyclic aromatic hydrocarbons from ex situ catalytic fast pyrolysis of pine over the HZSM-5 catalyst with calcium format as a hydrogen source. Sustain Energy Fuels 4:538–548. https://doi.org/10.1039/C9SE00605B

10. Prins MJ, Ptasinski KJ, Janssen FJJG (2006) More efficient biomass gasification via torrefaction. Energy 31:3458–3470. https://doi.org/10.1016/j.energy.2006.03.008

11. Recari J, Berrueco C, Puy N, Alier S, Bartroli J, Farriol X (2017) Torrefaction of a solid recovered fuel (SRF) to improve the fuel properties for gasification processes. Appl Energy 203:177–188. https://doi.org/10.1016/j.apenergy.2017.06.014

12. Pimchuai A, Dutta A, Basu P (2010) Torrefaction of agriculture residue to enhance combustible properties. Energy Fuels 24:4638–4645. https://doi.org/10.1021/ef901168f

13. Rousset P, Aguiar C, Labbe N, Commandre JM (2011) Enhancing the combustible properties of bamboo by torrefaction. Bioresour Technol 102:8225–8231. https://doi.org/10.1016/j.biortech.2011.05.093

14. Chen D, Chen F, Cen K, Cao X, Zhang J, Zhou J (2020) Upgrading rice husk via oxidative torrefaction: characterization of solid, liquid, gaseous products and a comparison with non-oxidative torrefaction. Fuel 275:117936. https://doi.org/10.1016/j.fuel.2020.117936

15. Ibrahim RHH, Darvell LI, Jones JM, Williams A (2013) Physicochemical characterisation of torrefied biomass. J Anal Appl Pyrol 103:21–30. https://doi.org/10.1016/j.jaap.2012.10.004

16. Ciolkosz D, Wallace R (2011) A review of torrefaction for bioenergy feedstock production. Biofuels Bioprod Biorefining 5:317–329. https://doi.org/10.1002/bbb.275

17. Chen W-H, Zhuang Y-Q, Liu S-H, Juang T-T, Tsai C-M (2016) Product characteristics from the torrefaction of oil palm fiber pellets in inert and oxidative atmospheres. Bioresour Technol 199:367–374. https://doi.org/10.1016/j.biortech.2015.08.066

18. Huang Y-F, Cheng P-H, Chiueh P-T, Lo S-L (2017) Microwave torrefaction of leucaena to produce biochar with high fuel ratio and energy return on investment. Energy Procedia 105:35–40. https://doi.org/10.1016/j.jtice.2016.10.056

19. Acharjee TC, Coronella CJ, Vasquez VR (2011) Effect of thermal pre-treatment on equilibrium moisture content of lignocellulosic biomass. Bioresour Technol 102:4849–4854. https://doi.org/10.1016/j.biortech.2011.01.018

20. Colin B, Dirion JL, Arlabosse P, Salvador S (2017) Quantification of the torrefaction effects on the grindability and the hygroscopicity of wood chips. Fuel 197:232–239. https://doi.org/10.1016/j.fuel.2017.02.028

21. Wang SR, Dai GX, Ru B, Zhao Y, Wang XL, Xiao G (2017) Influence of torrefaction on the characteristics and pyrolysis behavior of cellulose. Energy 120:864–871. https://doi.org/10.1016/j.energy.2016.11.135

22. Wang SR, Dai GX, Ru B, Zhao Y, Wang XL, Zhou JS (2016) Effects of torrefaction on hemicellulose structural characteristics and pyrolysis behaviors. Bioresour Technol 218:1106–1114. https://doi.org/10.1021/acs.energyfuels.7b03038

23. Arias B, Pevida C, Fermoso J, Plaza MG, Rubiera F, Pis JJ (2008) Influence of torrefaction on the grindability and reactivity of woody biomass. Fuel Process Technol 89:169–175. https://doi.org/10.1016/j.fuproc.2007.09.002

24. Phanphanich M, Mani S (2011) Impact of torrefaction on the grindability and fuel characteristics of forest biomass. Bioresour Technol 102:1246–1253. https://doi.org/10.1016/j.biortech.2010.08.028

25. Tapasvi D, Khalil R, Skreiberg O, Tran KQ, Gronli M (2012) Torrefaction of Norwegian birch and spruce: an experimental study using macro-TGA. Energy Fuels 26:5232–5240. https://doi.org/10.1021/ef300993q

26. Bridgeman TG, Jones JM, Williams A, Waldron DJ (2010) An investigation of the grindability of two torrefied energy crops. Fuel 89:3911–3918. https://doi.org/10.1016/j.fuel.2010.06.043

27. Gil MV, García R, Pevida C, Rubiera F (2015) Grindability and combustion behavior of coal and torrefied biomass blends. Bioresour Technol 191:205–212. https://doi.org/10.1016/j.biortech.2015.04.117

28. Singh Rk, Sarkar A, Chakraborty JP (2019) Effect of torrefaction on the physicochemical properties of pigeon pea stalk (Cajanus cajan) and estimation of kinetic parameters. Renew Energy 138:805–819. https://doi.org/10.1016/j.renene.2019.02.022

29. Pradhan P, Mahajani SM, Arora A (2018) Production and utilization of fuel pellets from biomass: a review. Fuel Process Technol 181:215–232. https://www.x-mol.com/paperRedirect/843446. Accessed 1 Dec 2018

30. Paulauskas R, Striugas N, Zakarauskas K, Dziugys A, Vorotinskiene L (2018) Investigation of regularities of pelletized biomass thermal deformations during pyrolysis. Therm Sci 22:603–612. https://doi.org/10.2298/TSCI160916090P

31. Shang L, Nielsen NPK, Dahl J, Stelte W, Ahrenfeldt J, Holm JK (2012) Quality effects caused by torrefaction of pellets made from Scots pine. Fuel Process Technol 101:23–28. https://doi.org/10.1016/j.fuproc.2012.03.013

32. Larsson SH, Rudolfsson M, Nordwaeger M, Olofsson I, Samuelsson R (2013) Effects of moisture content, torrefaction temperature, and die temperature in pilot scale pelletizing of torrefied Norway

spruce. Appl Energy 102:827–832. https://doi.org/10.1016/j.apenergy.2012.08.046

33. Basu P, Rao S, Acharya B, Dhungana A (2013) Effect of torrefaction on the density and volume changes of coarse biomass particles. Can J Chem Eng 91:1040–1044. https://doi.org/10.1002/cjce.21817

34 Kumar L, Tooyserkani Z, Sokhansanj S, Saddler JN (2012) Does densification influence the steam pretreatment and enzymatic hydrolysis of softwoods to sugars? Bioresour Technol 121:190–198. https://doi.org/10.1016/j.biortech.2012.06.049

35. Goh CS, Junginger M, Cocchi M, Marchal D, Thran D, Hennig C, HeinimoL J, Nikolaisen PP, Schouwenberg D, Bradley Hess R (2013) Wood pellet market and trade: a global perspective. Biofuels Bioprod Biorefining 7(1):24–42. https://doi.org/10.1002/bbb.136

36 Uslu A, Faaij AP, Bergman PC (2008) Pre-treatment technologies and their effect on International bioenergy supply chain logistics. Techno-economic evaluation of torrefaction, fast pyrolysis and palletisation. Energy 33(8):1206–1223. https://doi.org/10.1016/j.energy.2008.03.007

37. Ghiasi B, Kumar L, Furubayashi T, Jim Lim C, Bi X, Kim CS, Sokhansanj S (2014) Densified biocoal from woodchips: Is it better to do torrefaction before or after densification? Appl Energy 134:133–142. https://doi.org/10.1016/j.apenergy.2014.07.076

38. Yang Y, Sun Mm, Zhang M, Ke Z, Wang D, Lei C (2019) A fundamental research on synchronized torrefaction and pelleting of biomass. Renew Energy 142:668–676. https://doi.org/10.1016/j.renene.2019.04.112

39. Liu Zg, Quek A, Balasubramanian R (2014) Preparation and characterization of fuel pellets from woody biomass, agro-residues and their corresponding hydro chars. Appl Energy 113:1315–1322. https://doi.org/10.1016/j.apenergy.2013.08.087

40. Zhang Y, Chen F, Chen D, Cen K, Zhang J, Cao X (2020) Upgrading of biomass pellets by torrefaction and its influence on the hydrophobicity, mechanical property, and fuel quality. Biomass Conversion Biorefinery 18:1–10. https://doi.org/10.1007/s13399-020-00666-5

41. Lkhagvadorj Sh, Lee B-H, Jeong T-Y, Jeon C-H (2020) Effects of different pre-treatment methods on the grindability of pitch pine sawdust biomass and its blends with coal. J Mech Sci Technol 34:2235–2243. https://doi.org/10.1007/s12206-020-0445-4

42. Okot DK, Bilsborrow PE, Phan AN (2018) Effects of operating parameters on maize COB briquette quality. Biomass Bioenergy 112:61–72. https://doi.org/10.1016/j.biombioe.2018.02.015

43. Wilaipon P (2009) The effects of briquetting pressure on bananapeel briquette and the banana waste in Northern Thailand. Am J Appl Sci 6:167–171. https://doi.org/10.3844/ajassp.2009.167.171

44. Barta-Rajnai E, Wang L, Sebestyén Z, Barta Z, Khalil R, Skreiberg Ø, Grønli M, Jakab E, Czégény Z (2017) Effect of temperature and duration of torrefaction on the thermal behavior of stem wood, bark, and stump of spruce. Energy Procedia 105:551–556. http://creativecommons.org/licenses/by-nc-nd/4.0/. Accessed May 2017

45. Conag AT, Villahermosa JER, Luis K, Cabatingan, Go AW (2018) Energy densification of sugarcane leaves through torrefaction under minimized oxidative atmosphere. Energy Sustain Dev 42:160–169. https://doi.org/10.1016/J.ESD.2017.11.004

46. Pimchuai A, Dutta A, Basu P (2010) Torrefaction of agriculture residue to enhance combustible properties. Energy Fuel 24:4638–4645. https://doi.org/10.1021/ef901168f

47. C. Engineering Foundation (1994) The impact of ash deposition on coal fired plants, In: Proceedings of the Engineering Foundation Conference Held at the St. John's Swallow Hotel, Solihull, England, June 20–25, 1993, Taylor & Francis, [1994] ©1994, Washington, DC

48. Strandberg M, Olofsson I, Pommer L, Wiklund-Lindströma S (2015) Effects of temperature and residence time on continuous torrefaction of spruce wood. Fuel Process Technol 134:387–398. https://doi.org/10.1016/j.fuproc.2015.02.021

49. Åberg K, Nordin A (2008) GREET life cycle model, GREET transportation fuel cycle analysis model, GREET 1.8b. Argonne Natl. Lab. Copyr. 2012 Chicago Argonne, LLC. http://greet.es.anl.gov/. Accessed 2020-10-09

50. Singh D, Yadav S (2019) Evaluation of the physico-chemical development of kitchen food wastes through torrefaction a biodiversity case study. Biomass Convers Biorefin.https://doi.org/10.1007/s13399-019-00526-x

51. Xu F, Yu J, Tesso T, Dowell F, Wang D (2013) Qualitative and quantitative analysis of lignocellulosic biomass using infrared techniques: a mini-review. Appl Energy 104:801–809. https://doi.org/10.1016/j.apenergy.2012.12.019

52. Sills DL, Gossett JM (2012) Using FTIR to predict saccharification from enzymatic hydrolysis of alkali pre-treated biomasses. Biotechnol Bioeng 109:353–362. https://doi.org/10.1002/bit.23314

53. Schwanninger M, Rodrigues J, Pereira H, Hinterstoisser B (2004) Effects of short time vibratory ball milling on the shape of FT-IR spectra of wood and cellulose. Vib Spectroscopy 36:23–40. https://doi.org/10.1016/j.vibspec.2004.02.003

54. Kubo S, Kadla JF (2005) Hydrogen bonding in lignin: a Fourier transforms infrared model compound study. Biomacromolecules 6:2815–2821. https://doi.org/10.1021/bm050288q+

55. Sadaka S, Negi S (2009) Improvements of biomass physical and thermochemical characteristics via torrefaction process. Environ Prog Sustain Energy 28(3):427–434. https://doi.org/10.1002/ep.10392

56. Bridgeman TG, Jones JM (2008) Torrefaction of reed canary grass, wheat straw and willow to enhance solid fuel qualities and combustion properties. Fuel:844–56.https://doi.org/10.1016/j.fuel.2007.05.041

57. González-Peña MM, Hale MD (2009) Colour in thermally modified wood of beech, Norway spruce and Scots pine. Part 1: colour evolution and colour changes. Holzforschung 63:385–393. https://doi.org/10.1515/HF.2009.078

58. Gil MV, Oulego P, Casal MD, Pevida C, Pis JJ, Rubiera F (2010) Mechanical durability and combustion characteristics of pellets from biomass blends. Bioresour Technol 101:8859–8867. https://doi.org/10.1016/j.biortech.2010.06.062

59. Rousset P, Lapierre C, Perré P, Quirino W (2009) Effect of severe thermal treatment on spruce and beech wood lignins. Ann Forest Sci 66:110–118. https://doi.org/10.1051/forest/2008078

60. Kaliyan N, Morey RV (2009) Factors affecting strength and durability of densified biomass products. Biomass Bioenergy 33:337–359. https://doi.org/10.1016/j.biombioe.2008.08.005

61. Chen WH, Peng J, Bi XT (2015) A state-of-the-art review of biomass torrefaction, densification and applications. Renew Sustain Energy Rev 44:847–866. https://doi.org/10.1016/j.rser.2014.12.039

62. Nanou P, Huijgen WJJ, Carbo MC, Kiel JHA (2018) The role of lignin in the densification of torrefied wood in relation to the final product properties. Biomass Bioenergy 111:248–262. https://doi.org/10.1016/j.biombioe.2017.05.005

63. Jakub S, Marek W, Jarosław F, Adrian K (2020) Effect of compaction pressure and moisture content on quality parameters of perennial biomass pellets. Energies 13:1859. https://doi.org/10.3390/en13081859

64. Abedin Z, Mohammad HK (2012) Effect of temperature, pressure and moisture content on durability of cattle manure pellet in open-end die method. J Agric Sci 4:203–208. https://doi.org/10.5539/jas.v4n5p203

65. Esteves B, Marques V, Domingos A, Pereira IH (2008) Heat-induced colour changes of pine (Pinus pinaster) and eucalypt (Eucalyptus globulus) wood. Wood Sci Technol 42:369–384. https://doi.org/10.1007/s00226-007-0157-2

66. Järvinen T, Agar D (2014) Experimentally determined storage and handling properties of fuel pellets made from torrefied whole-tree pine chips, logging residues and beech stem wood. Fuel 129:330–339. https://doi.org/10.1016/j.fuel.2014.03.057

67. Tanno K, Makino H (2018) Development Tendency and Prospect of High-Performance Coal Utilization Power Generation System for Low Carbon Society. KONA Powder and Particle Journal No 35, 139:149. https://doi.org/10.14356/kona.2018021

68. Ohm TI, Chae JS, Kim JK, Oh SC (2015) Study on the characteristics of biomass for co-combustion in coal power plant. J Mater Cycles Waste Manag 17:249–257. https://doi.org/10.1007/s10163-014-0334-y

69. European Pellet Council Version 3.0 (2015) ENplus Handbook (UK Pellet council-Hand book), Part 3 - Pellet Quality Requirements, EPC. http://www.enplus-pellets.eu/

70. Verhoest C, Ryckmans Y (2012) Industrial wood pellets report, In: Laborelec (ed) Laborelec & Pellcert. http://www.enpluspellets.eu/wp-content/uploads/2012/04/Industrial-pellets-report_PellCert_2012_secured.pdf

71. Jian D, Wang G-j, Kuang J-h, Zhang Y-l, Luo Y-h (2009) Pretreatment of agricultural residues for co-gasification via torrefaction. J Anal Appl Pyrolysis 86:331–337. https://doi.org/10.1016/j.jaap.2009.08.006

72. Chen D, Zheng Z, Fu K, Zeng Z, Wang J, Lu M (2015) Torrefaction of biomass stalk and its effect on the yield and quality of pyrolysis products. Fuel 159:27–32. https://doi.org/10.1016/j.fuel.2015.06.078

73. Obinna OB, Kingsley ES, Okwuchukwu M (2016) Torrefaction of Nigerian palm kernel shell into solid fuel. Sci Innov 4(3–1):19–23. https://doi.org/10.11648/j.si.s.2016040301.13

74. Jes T, De Leon R (2018) Solid fuel characterization of torrefied coconut shells in an oxidative environment. Int J Smart Grid Clean Energy 7(2):145–151. https://doi.org/10.12720/sgce.7.2.145-151